

This is the accepted manuscript made available via CHORUS. The article has been published as:

Spin excitations in $K_{\{2\}}Fe_{\{4+x\}}Se_{\{5\}}$: Linear response approach

Liqin Ke, Mark van Schilfgaarde, and Vladimir Antropov

Phys. Rev. B **86**, 020402 — Published 17 July 2012

DOI: [10.1103/PhysRevB.86.020402](https://doi.org/10.1103/PhysRevB.86.020402)

Spin excitations in $\text{K}_2\text{Fe}_{4+x}\text{Se}_5$: linear response approach

Liqin Ke,¹ Mark van Schilfgaarde,² and Vladimir Antropov¹

¹*Ames Laboratory USDOE, Ames, IA 50011*

²*Department of Physics, King's College London, Strand, London WC2R 2LS*

(Dated: June 27, 2012)

Using *ab initio* linear response techniques we calculate spin wave spectra in $\text{K}_2\text{Fe}_{4+x}\text{Se}_5$, and find it to be in excellent agreement with a recent experiment. The spectrum can be described reasonably well by localized spin Hamiltonian restricted to first and second nearest neighbor couplings. We confirm that exchange coupling between nearest neighbor Fe magnetic moments is strongly anisotropic, and show directly that in the ideal system this anisotropy has itinerant nature which can be imitated by introducing higher order terms in effective localized spin Hamiltonian (biquadratic coupling). In the real system, structural relaxation provides an additional source of the exchange anisotropy of approximately the same magnitude. The dependence of spin wave spectra on filling of Fe vacancy sites is also discussed.

PACS numbers: PACS number

Because there seems to be a close, if poorly understood, connection between magnetic excitations and superconductivity in the recently discovered families of Fe-based superconductors, a great deal of attention has been paid to the elementary magnetic excitations in these systems^{1,2}. While the number of materials with superconducting properties is rapidly growing, they all share in common a phase diagram with an antiferromagnetic region immediately adjacent to the superconducting phase. AFM order in most parent compounds are characterized by rather steep spin waves (antiferromagnons) and relatively low Néel temperature ($\sim 140\text{ K}$)^{1,2}. On the other hand, iron selenides $\text{K}_2\text{Fe}_{4+x}\text{Se}_5$ discovered very recently, which we will call here a “245” system, is a particularly interesting case, because while its superconducting state appears to be similar in many respects to some of the other families, it has a much higher Néel temperature ($T_N \sim 560\text{ K}$) and very large magnetic moment ($\sim 3\mu_B$)^{3–5}. The first neutron experiments, performed only recently⁶, show collective spin excitations somewhat similar to excitations in the Fe-pnictides such as CaFe_2As_2 . A highly debated topic of discussion is the anisotropy of the exchange coupling. In Ref.⁶ the authors fit a set of anisotropic Heisenberg model parameters to their data, and argued that at least three effective nearest neighbor (NN) exchange parameters are needed to fit observed spectra in a satisfactory manner. In another recent work⁷ this exchange anisotropy has been fully attributed to biquadratic exchange, supporting the model introduced in Ref.⁶. However, neutron linear response experiments do not contain sufficient information to establish whether or not higher order terms of localized spin Hamiltonian or other interactions are responsible for this anisotropy. Information from the linear regime cannot unambiguously distinguish the dependence of linear response behavior on environment and terms originating from higher order. The unique answer can be obtained using non-collinear band structure calculations together with a linear response theory⁸.

Here we analyze spin excitations in the 245 system

using non-collinear density functional theory in tandem with a linear response approach to determine the spin wave (SW) spectra of both the parent compound, $\text{K}_2\text{Fe}_4\text{Se}_5$, and its modification by addition of Fe on the ‘vacancy’ sites. We accurately reproduce observed features in SW spectra of the parent compound from this first principles approach, without recourse to empirical or adjustable parameters. Thus we argue that the Heisenberg model extracted from this theory provides a good description of the static transverse susceptibility, and the exchange parameters J_{ij} derived *ab initio* from it, which have a physical meaning as the second variation in total energy with respect to spin rotations. We can also unambiguously address what happens when exchange parameters, which can be computed to whatever range is desired, are truncated to a short range, e.g. just first and second neighbors (J_1 – J_2 model).

For computational convenience we adopt a multiple-scattering approach in the long wave approximation⁹, which is reasonable provided the local Fe moment is sufficiently large. This is the case in $\text{K}_2\text{Fe}_{4+x}\text{Se}_5$ ^{10,11}, where the Fe local moment is both measured to be $\sim 3\mu_B$, and predicted to be so in density-functional theory.

The parent compound $\text{K}_2\text{Fe}_4\text{Se}_5$ has a vacancy on the Fe sublattice for each formula unit, which if filled would have a composition $\text{K}_2\text{Fe}_5\text{Se}_5$ and be structurally similar to the other Fe superconductors. The ordered magnetic phase of $\text{K}_2\text{Fe}_4\text{Se}_5$ is unusual: blocks of four Fe atoms are coupled ferromagnetically in a square; the squares are arranged antiferromagnetically in a Néel like configuration, which we denote the “block Néel” magnetic structure. In what manner the vacancy Fe sites are filled in superconducting material is a crucial issue, because the parent compound is predicted in density-functional theory to be an insulator with a bandgap of $\sim 0.4\text{ eV}$ ¹².

We first consider magnetic excitations of the parent compound, with reciprocal lattice vectors $G_1=(0.4,-0.2,0)$, $G_2=(0.2,0.4,0)$, and $G_3=(0,0,a/c)$, in units of $2\pi/a$. This cell contains four formula units of $\text{K}_2\text{Fe}_4\text{Se}_5$ with two units per plane. We used exper-

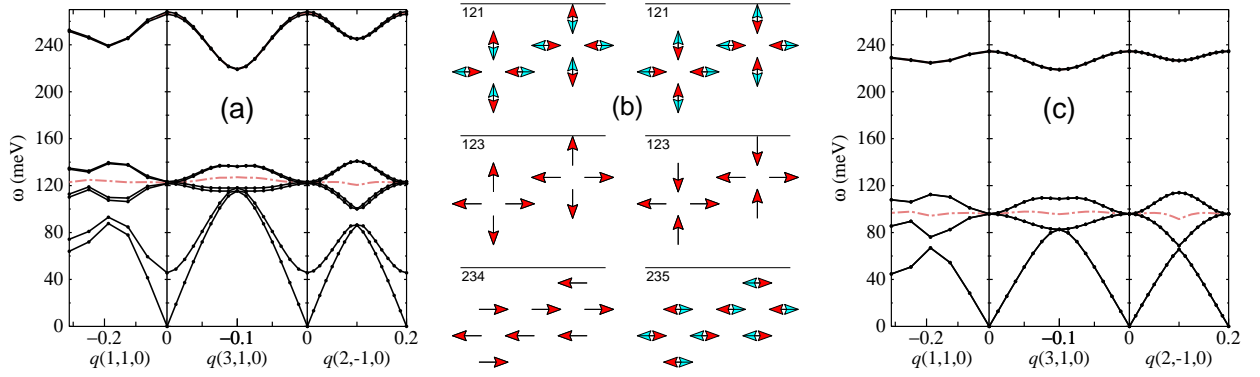


FIG. 1: Spin-wave spectra in $\text{K}_2\text{Fe}_4\text{Se}_5$ calculated from the static susceptibility in the LDA. Panel (a) shows $\omega(q)$, with the right frame for q along the $\Gamma-G_1$ line. It corresponds to the experimental spectra shown in Ref.⁶ (bottom panels of Fig. 3), whereas the left frame corresponds to the top panel of that Figure. The middle frame shows spectra along the $\Gamma-(G_1+G_2)$ line. Panel (b) shows eigenvectors of the six optical modes at Γ , and their corresponding frequencies (meV). The perspective is from the z axis, so each point contains two Fe atoms. Arrows correspond to spin rotations of each of the 16 Fe atoms. In some panels only 8 arrows are visible; this occurs when the rotations in the upper and lower planes are in phase. In other panels all 16 arrows are visible; for these modes the lower and upper planes are 180° out of phase. The right frame shows how the SW get modified when exchange interactions are restricted to J_1 and J_2 only.

TABLE I: Bond lengths (\AA) of $\text{K}_2\text{Fe}_4\text{Se}_5$ in the block Néel structure calculated from PBE and LDA functionals, bandgap E_g (eV) and magnetic moment M (μ_B). “LDA@PBE” refers to calculations using the Barth-Hedin (local) functional, but calculated at the PBE minimum-energy geometry. The shorter (longer) of the Fe-Fe bond length is the intrablock (interblock) distance. Mean PBE Fe-Fe and Fe-Se bond lengths are close to the experimental values. “25% Fe” refers to an LDA@PBE calculation with 25% doping of the Fe vacancy sites, as discussed in the text.

	$d(\text{Fe-Fe})$	$d(\text{Fe-Se})$	E_g	M
Expt	2.768	2.441		3.3
PBE	2.657–2.901	2.406–2.509	0.59	3.02
LDA	2.649–2.872	2.354–2.454	0.26	2.75
LDA@PBE			0.44	2.90
25% Fe	2.604–2.814	2.399–2.518	0.01	2.3–2.9

imental lattice constants from Ref.¹³ with $a=3.914\text{\AA}$, and $c/a=3.587$. Because the LDA is known to underestimate Fe-chalcogen and Fe-pnictogen bond lengths in these families of superconductors, we use the PBE functional to relax the crystal structure in the block Néel magnetic state. The resulting relaxed structure (Table I) agrees well with experimental data. On the other hand, the PBE functional tends to overestimate magnetic stabilization energy and moment M . Thus to calculate magnetic excitations, we use the LDA, but adopt the crystal structure predicted by the PBE functional.

The full susceptibility $\chi^{-1}(\mathbf{q}, \omega)$ is prohibitively expensive to calculate for such a large system. Thus we adopt an approach which relies on the atomic sphere approximation (ASA) following Ref.¹⁴. To check the ASA approximation to DFT we carefully checked the ASA energy bands, density of states, and magnetic moment M against LDA results and found satisfactory agreement

for all cases described here; for example E_g and M of $\text{K}_2\text{Fe}_4\text{Se}_5$ were found to be 0.40 eV and $2.85\mu_B$, close to the LDA@PBE result of Table I.

Pair exchange parameters J_{ij} were obtained from a Fourier transform of $J(\mathbf{q})$; the latter was calculated on fine a q -mesh of $16 \times 16 \times 4$ divisions in order to reliably extract J_{ij} to very distant neighbors. Resulting spin wave spectra for the parent compound $\text{K}_2\text{Fe}_4\text{Se}_5$ are shown in Fig. 1. Focusing first on the Γ point, six optical modes are seen: two nearly degenerate pairs clustered around 120 meV, and another near 40 meV. (We defer discussion of the mode near 40 meV for the moment.) Panel (b) of Fig. 1 depicts their eigenvectors. The four eigenmodes near 120 meV consist of the following. There are two energetically equivalent kinds of motion in a plane normal to z (middle modes of Fig. 1(b)) Each kind has one eigenmode with spins in $z=0$ planes and $z=c/2$ planes precessing in phase (123 meV), and a 121 meV mode with precession out of phase (top modes of Fig. 1(b)). The 234 meV and 235 meV modes are similarly related.

Left and right frames can be compared directly with neutron data, top and bottom panels of Fig. 3 of Ref.⁶. All modes match experimental data very well, when broadening in the experimental spectrum is taken into account. The acoustic mode, with linear dispersion for small q of Fig. 1 has a maximum of 86 meV at $q=(1/2)G_1$, slightly larger than the measured value in Ref.⁶. The four low-energy optical modes are all “breathing” modes: spins rotate radially away from the center of their square. These four separate modes cannot be resolved in experiment; instead the measured data reflects a superposition of these modes. It is nearly dispersionless along the $\Gamma-G_1$ line, with $\omega \approx 110$ meV. The four optical modes were averaged and shown as a dashed line in Fig. 1, and the result is seen to be similar to the neutron data, though at slightly higher energy. Finally the two high-

TABLE II: Exchange energies J_k , in meV, for the Heisenberg hamiltonian $H = \sum J_{ij} \mathbf{S}_i \cdot \mathbf{S}_j$, of the parent compound $\text{K}_2\text{Fe}_4\text{Se}_5$. Here k denotes the neighbor index. J_k and J'_k refer to couplings between pairs of like spin and opposite spin, respectively. Also shown is the Néel temperature, estimated from the RPA¹⁵.

k	Relaxed geometry		Ideal geometry	
	J_k	J'_k	J_k	J'_k
1	-9.7	27.3	-5.7	25.7
2	10.2	8.5	17.0	6.7
3	0.3	-0.3	0.1	-0.1
4	-1.9	0.1 \pm 1.0	-2.2	0.5 \pm 0.5
5	0.1	0.5	-0.3	0.5
6	-0.1	0.1 \pm 0.1		0.1 \pm 0.1
7	-0.1	1.3		
T_N	494 K		(not stable)	

energy optical modes show a weak q dependence, with $\omega \approx 240$ meV. Essentially identical behavior is observed in the neutron data along the (110) line, though ω is slightly smaller. The Néel temperature, T_N , estimated within the RPA, is about 12% smaller than the observed value. This is in fact very good agreement with experiment, since the RPA is known to underestimate critical temperatures for a given Hamiltonian, by roughly 10%.

Finally, consider the mode appearing near 40 meV. If the two Fe planes were identical and uncoupled this mode would exactly coincide with the acoustic mode. Thus it is essentially the acoustic mode with $q_z = 1/2 \cdot 2\pi/c$, zone-folded to the Γ point, because the actual crystal contains two planes of Fe. The splitting of this and the true acoustic mode are a result of coupling between the two planes through exchange parameters along J^z coupling different planes. This shows that J^z is small, but not so small that planes are decoupled.

A great deal of speculation has arisen about the size and range of parameters J . Much effort has been expended extracting effective exchange parameters J_{ij} by fitting a Heisenberg model with a few (2 or 3) neighbors to the observed data, as was done in Refs.⁶ and ⁷. Since as we have shown, SW are well described by the Heisenberg model derived *ab initio*, the model can be used to unambiguously address questions about the range and environment dependence of J_{ij} . In particular, it is debated whether a J_1 - J_2 model is sufficient or more distant neighbors are required. Table II shows J_{ij} for the first few neighbors, distinguishing intra-block and inter-block couplings. As widely thought, the first two neighbors give by far the largest contribution to J . To quantify this effect, we recalculated the SW spectrum with J restricted to only nearest and second neighbor. This leaves four independent parameters since interblock J and intrablock J' are distinct (Table II). The resulting SW spectra, shown in the right panel of Fig. 1, look qualitatively similar to the full calculation, except that some modes become degenerate, and low-energy modes soften by about 25%. The predicted T_N drops by a comparable amount, from 494K to 399K. Perhaps most importantly,

the “zone-folded” acoustic mode noted above becomes degenerate with the true acoustic mode, because all interplane interactions are now excluded by construction.

Remarkably, corrections to the J_1 - J_2 approximation receive almost *no* contribution from J_3 ; rather, they originate from J_4 - J_7 (note J'_7). The magnetic structure is stabilized by strong AFM first and second neighbor interblock coupling, and weakly so by nearest intrablock exchange. Frustration is present, since the AFM second neighbor intrablock coupling acts strongly to destabilize the magnetic order, but it is overcome because there are half as many such pairs as their interblock counterparts. The Table also shows what J_{ij} would obtain if the structure were constrained to an ideal geometry. Relaxation causes a small deformation of the Fe atoms in squares; there is also some dispersion in the Fe-Se bond length around the average value (Table I). This structural relaxation is critically important for magnetic stability. As Table II shows, the stability of the (intrablock) square is strongly enhanced by relaxation: the NN coupling is increased and frustration in the 2nd NN is strongly reduced. Without relaxation some of SW frequencies become complex, indicating that the collinear state is not stable.

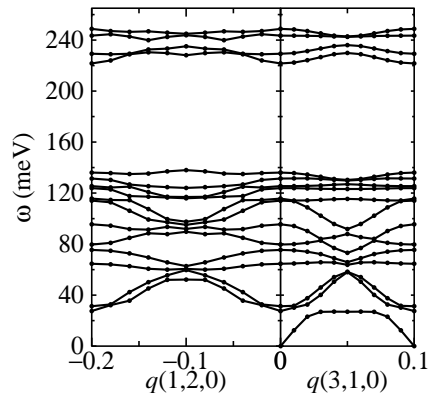


FIG. 2: Spin-wave spectra for $\text{K}_2\text{Fe}_{4.25}\text{Se}_5$ as described in the text. Actual cell is $\text{K}_{16}\text{Fe}_{34}\text{Se}_{40}$, which is twice as large as the cell used in Fig. 1.

As the filling of Fe vacancy sites very likely play an essential role in mediating superconductivity, how elementary excitations are modified when these sites are partially occupied is a crucial question. We consider now 25% occupation of Fe vacancy sites. To retain an overall zero-spin configuration it is necessary to double the size of the four formula unit cell: we construct a supercell with $G_1 = (0.3, 0.1, 0)$ and $G_2 = (-0.1, 0.3, 0)$, and populate two of the eight vacancy sites with a pair of Fe^\uparrow and Fe^\downarrow atoms in such a way as to preserve a two-fold rotational symmetry. The lattice was relaxed using the PBE functional, with the resulting equilibrium bond lengths shown in Table I. SW's are shown in Fig. 2. The acoustic mode (now zone folded) is largely unchanged and uncoupled from the other modes: there is a linear dispersion at small q and a maximum near 80 meV for, e.g. $\mathbf{q} = (0.3, 0.1, 0)$

and $\mathbf{q}=(0.1, -0.2, 0)$. The (zone-folded) low-energy optical modes show some new features. In addition to the modes in the 80-120 meV range, new and largely dispersionless modes appear around 60 meV. The eigenfunctions of these modes are very complex, with strong admixtures of both vacancy sites and host sites. The high-frequency modes are almost unchanged as “vacancy” Fe atoms participate very little in them.

At 25% filling the magnetic structure is stable; indeed T_N for $\text{K}_2\text{Fe}_4\text{Se}_5$, predicted to be 494 K in the Tyablikov approximation, is only slightly reduced, to 485 K for $\text{K}_2\text{Fe}_{4.25}\text{Se}_5$. We also studied a case with 50% filling. A collinear magnetic state was stabilized; however the linear response calculation of the SW spectra revealed imaginary frequencies, indicating that the collinear state is not stable.

The exchange anisotropy, $J_k - J'_k$, is unusually large in this material. It is natural to associate $J_k - J'_k$ with biquadratic coupling, as was done in Refs.¹⁶. However, lattice relaxations are very important in this case; compare the ideal to relaxed J in Table II. Our calculations predict that the intrablock NN Fe-Fe bond length smaller than the intrablock one by $\sim 8\%$ (Table I); and perhaps more important, there is a significant dispersion in the Fe-Se bond lengths. The strictly electronic (relaxation-independent) part of biquadratic contribution is still present, but it is cumbersome to calculate. We estimated the biquadratic contribution to a weighted average of J_1 and J'_1 by rotating the four spins centered around a vacancy to large angles (this collective rotation preserves angles between second neighbors), and fitting the total energy to an effective spin Hamiltonian with higher order terms. We found that more than half of the effective J_1 obtained from linear response originates from the biquadratic contribution. Thus the environment dependence of J originates from two sources: purely electronic terms for a fixed lattice, and an “exchange-striction” con-

tribution, originating from spin-configuration-dependent lattice relaxation. (The decomposition is somewhat arbitrary, as it depends on how “relaxation” is defined¹⁷.)

These non-collinear calculations point to the microscopic origin of the biquadratic interaction. It appears that major contribution to this ‘biquadratic’ energy is produced by the change of the amplitude of magnetic moments. M was found to vary by $\sim 0.3\mu_B$, even though its magnitude is large and thought to be well described by a rigid local-moment picture. The unusually large interaction between longitudinal and transverse degrees of freedom reflects the relatively large itinerant component of magnetic interactions in this system. It is notable that the interaction between these kinds of fluctuations lies outside a linear response description. The LDA is a mean-field theory and does not incorporate fluctuations directly. It can nevertheless capture some aspect of fluctuations through the imposition of constraints (spin orientations).

In conclusion, we demonstrated that *ab-initio* linear response method nearly perfectly describes the observed spin wave spectra in the complicated 245 system. A localized spin Hamiltonian restricted to two nearest neighbor couplings is sufficient to describe the full calculation reasonably well. We confirm the anisotropy of the exchange coupling between NN Fe magnetic moments and established that this anisotropy is associated with significant biquadratic coupling which appears in part because of longitudinal fluctuations. Structural relaxation provides an additional source of the exchange anisotropy of approximately the same magnitude.

Work at the Ames Laboratory was supported by DOE Basic Energy Sciences, Contract No. DE-AC02-07CH11358. We thank the July, 2011 Aspen Center for Physics workshop on superconductivity for the opportunity to do this research (NSF Grant 1066293).

¹ D. C. Johnston, *Advances in Physics* **59**, 803 (2010).

² J. W. Lynn and P. Dai, *Physica C: Superconductivity* **469**, 469 (2009).

³ W. Bao, G. N. Li, Q. Huang, G. F. Chen, J. B. He, M. A. Green, Y. Qiu, D. M. Wang, and J. L. Luo, *ArXiv e-prints* (2011), 1102.3674.

⁴ P. Zavalij, W. Bao, X. F. Wang, J. J. Ying, X. H. Chen, D. M. Wang, J. B. He, X. Q. Wang, G. F. Chen, P.-Y. Hsieh, et al., *Phys. Rev. B* **83**, 132509 (2011).

⁵ B. Wei, H. Qing-Zhen, C. Gen-Fu, M. A. Green, W. Du-Ming, H. Jun-Bao, and Q. Yi-Ming, *Chin. Phys. Lett.* **28**, 086104 (2011).

⁶ M. Wang, C. Fang, D.-X. Yao, G. Tan, L. W. Harriger, Y. Song, T. Netherton, C. Zhang, M. Wang, M. B. Stone, et al., *Nature Commun.* **2**, 580 (2011).

⁷ J. Hu, B. Xu, W. Liu, N.-N. Hao, and Y. Wang, *Phys. Rev. B* **85**, 144403 (2012).

⁸ T. Kotani and M. van Schilfgaarde, *J. Phys.: Condens. Matter* **20**, 295214 (2008).

⁹ V. Antropov, *J. Magn. Magn. Mater.* **262**, L192 (2003).

¹⁰ D. Mou, L. Zhao, and X. Zhou, *Frontiers of Physics* **6**, 410 (2011).

¹¹ While neutron measurements were made for $\text{Rb}_2\text{Fe}_4\text{Se}_5$, Rb and K play very similar roles, so that the spin excitation (dominated by Fe) should be also similar.

¹² C. Cao and J. Dai, *Phys. Rev. Lett.* **107**, 056401 (2011).

¹³ Z. Wang, Y. J. Song, H. L. Shi, Z. W. Wang, Z. Chen, H. F. Tian, G. F. Chen, J. G. Guo, H. X. Yang, and J. Q. Li, *Phys. Rev. B* **83**, 140505 (2011).

¹⁴ M. van Schilfgaarde and V. P. Antropov, *J. Appl. Phys.* **85**, 4827 (1999); V. P. Antropov, M. van Schilfgaarde, S. Brink, and J. L. Xu, *J. Appl. Phys.* **99**, 08F507 (2006).

¹⁵ V. Antropov, B. Harmon, and A. Smirnov, *J. Magn. Magn. Mater.* **200**, 148 (1999).

¹⁶ J. Pulikotil, L. Ke, M. van Schilfgaarde, T. Kotani, and V. Antropov, *Superconductor Science and Technology* **23**, 054012 (2010); A. L. Wysocki, K. D. Belashchenko, and V. P. Antropov, *Nature Phys.* **7**, 485 (2011).

¹⁷ By “unrelaxed” we mean that all Fe atoms occupy sites on an ideal square lattice; the K and Se atoms are allowed to relax to their minimum-energy configuration.